Received: 19 March 2021 | Accepted: 29 June 2021

DOI: 10.1002/prp2.891

ORIGINAL ARTICLE

Metabolism and disposition of opicapone in the rat and metabolic enzymes phenotyping

Ana I. Loureiro[1] | Carlos Fernandes-Lopes[1] | Maria João Bonifácio[1] | Filipa Sousa[1] | László E. Kiss[1] | Patricio Soares-da-Silva[1,2,3]

[1]Department of Research and Development, BIAL—Portela & Cª. S.A., S Mamede do Coronado, Portugal

[2]Unit of Pharmacology and Therapeutics, Department of Biomedicine, Faculty of Medicine, University of Porto, Porto, Portugal

[3]MedInUp—Center for Drug Discovery and Innovative Medicines, University of Porto, Porto, Portugal

Correspondence
Ana I. Loureiro, Department of Research and Development, BIAL, À Av. da Siderurgia Nacional, 4745-457 Coronado (S. Mamede and S. Romao), Portugal.
Email: ana.loureiro@bial.com

Funding information
BIAL—Portela & Cª, S.A.

Abstract

Opicapone (2,5-dichloro-3-(5-(3,4-dihydroxy-5-nitrophenyl)-1,2,4-oxadiazol-3-yl)-4,6-dimethylpyridine 1-oxide) is a selective catechol-O-methyltransferase inhibitor that has been granted marketing authorization in Europe, Japan, and United States. The present work describes the metabolism and disposition of opicapone in the rat obtained in support to its development and regulatory filling. Plasma levels and elimination of total radioactivity were determined after oral and intravenous administration of [^{14}C]-opicapone. The maximum plasma concentrations of opicapone-related radioactivity were reached at early time points followed by a gradual return to baseline with a biphasic elimination. Fecal excretion was the primary route of elimination of total radioactivity. Quantitative distribution of drug-related radioactivity demonstrated that opicapone and related metabolites did not distribute to the central nervous system. Opicapone was extensively metabolized in rats resulting in more than 20 phase I and phase II metabolites. Although *O*-glucuronidation, -sulfation, and -methylation of the nitrocatechol moiety were the principal metabolic pathways, small amount of the *N*-acetyl derivative was detected, as a result of reduction of the nitro group and subsequent conjugation. Other metabolic transformations included *N*-oxide reduction to the pyridine derivative and reductive cleavage of 1,2,4-oxadiazole ring followed by further conjugative reactions. Reaction phenotyping studies suggested that SULT 1A1*1 and *2 and UGT1A7, UGT1A8, UGT1A9, and UGT1A10 may be involved in opicapone sulfation and glucuronidation, respectively. However, the reductive metabolic pathways mediated by gut microflora cannot be excluded. Opicapone, in the rat, was found to be rapidly absorbed, widely distributed to peripheric tissues, metabolized mainly via conjugative pathways at the nitro catechol ring, and primarily excreted via feces.

Abbreviations: BCS, Biopharmaceutics Classification System; CMC, carboxymethylcellulose; CNS, central nervous system; COMT, catechol-*O*-methyltransferase; EMA, European Medicines Agency; FDA, Food and Drug Administration; GSH, glutathione; HIM, human intestinal microsomes; HLM, human liver microsomes; HPLC, high-pressure liquid chromatography; HPLC-ED, high-pressure liquid chromatography–electrochemical detector; HPMC, hydroxypropyl methylcellulose; LC–MS, liquid chromatography–mass spectrometry; MHLW, Ministry of Health Labor and Welfare; PAPS, adenosine 3′-phosphate 5′-phosphosulfate; PD, Parkinson's disease; PK, pharmacokinetics; QC, quality control; QWBPI, quantitative whole-body phosphor imaging; SULT, sulfotransferase; UDPGA, uridine 5'-diphospho-glucuronic acid; UGT, UDP-glucuronosyltransferase.

KEYWORDS
glucuronidation, metabolism, opicapone, pharmacokinetics, rat, sulfation

1 | INTRODUCTION

Opicapone is a reversible, peripherally selective, high binding affinity, and long-acting third generation nitrocatechol catechol-*O*-methyltransferase (COMT) inhibitor, devoid of cytotoxic effects,[1,2] and has been shown to reduce the peripheral metabolism of levodopa (the mainstay antiparkinsonian drug) to 3-*O*-methyl-levodopa,[3] and hereby improves motor response in Parkinson's disease (PD) patients.[4–12] Opicapone has recently been granted marketing authorization under the trade name Ongentys® by EMA, MHLW, and FDA, to be used in the adjunctive levodopa therapy of PD patients.

The pharmacokinetic profile of opicapone and its metabolites was investigated in healthy subjects demonstrating an approximately linear pharmacokinetics (PK) following single ascending oral doses (10, 25, 50, 100, 200, 400, 800, and 1200 mg)[13] and multiple once-daily oral doses.[14] Despite its short apparent terminal elimination half-life ($t_{1/2}$, 0.8–3.2 h), the levels of COMT inhibition in erythrocyte were sustained far beyond the observable point of plasma drug clearance (6–10 h) making it suitable for a once-daily dosage regimen.[14]

In contrast to other nitrocatechol COMT inhibitors, such as entacapone, tolcapone, or nebicapone—which are extensively metabolized by glucuronidation followed by rapid excretion in the urine[15–18]—only trace amounts of opicapone glucuronide derivative were detected in humans even at higher doses administered. While the *N*-oxide reduced derivative of opicapone was found to be another minor metabolite, the *O*-sulfate conjugate appeared to be the major metabolite of opicapone with a relatively long $t_{1/2}$, ranging from 25.1 to 26.9 h following a single dose and from 98.5 to 112.0 h following repeated dosing, respectively.[14] Sulfotransferase (SULT) and UDP-glucuronosyltransferase (UGT) are phase II metabolizing enzymes responsible for conjugative pathways that catalyze the addition of sulfate and glucuronic acid, respectively, to functional groups including aromatic hydroxyl groups.[19] Characterization of the SULT and UGT isoforms involved in a drug metabolism is essential to anticipate the potential for metabolism-mediated drug interactions and inter-individual variations in drug metabolism and PK. In this study, the metabolism and disposition of opicapone was investigated in the rat, in support to the opicapone drug development. Plasma levels and elimination of total radioactivity were determined after oral and intravenous administration of [^{14}C]-opicapone. The tissue distribution of [^{14}C]-opicapone was determined by quantitative whole-body phosphor imaging (QWBPI) and the biotransformation of opicapone was characterized in rat urine, plasma, and feces after oral administration of [^{14}C]-opicapone using accurate mass LC–MS combined with parallel offline radiodetection.

2 | MATERIALS AND METHODS

2.1 | Reagents

Unlabeled opicapone (BIA 9-1067; 2,5-dichloro-3-(5-(3,4-dihydroxy-5-nitrophenyl)-1,2,4-oxadiazol-3-yl)-4,6-dimethylpyridine 1-oxide) was supplied by BIAL as a yellow powder with a chemical purity of 98%. [^{14}C]-Opicapone (Figure 1), specific radioactivity 2.09 GBq/mmol (5.03 MBq/mg), was supplied by GE Healthcare UK and by Quotient Bioresearch, UK at a radiochemical purity of 99.1%. Opicapone metabolites were synthesized in the Laboratory of Chemistry, BIAL (Coronado [S. Mamede, S. Romao], Portugal [metabolite details in Supporting Information]). The uridine 5'-diphospho-glucuronic acid (UDPGA), Adenosine 3′-phosphate 5′-phosphosulfate (PAPS), magnesium chloride, and all other chemicals were purchased from Sigma-Aldrich. Recombinant human UGTs expressed in baculovirus-infected insect cells were purchased from PanVera-Invitrogen (Carlsbad, CA; 1A1, 1A3, 1A6, 1A7, 1A10, and 2B7) and from BD Biosciences (1A4, 1A8, 1A9, 2B15, 2B4, and 2B17). Pooled human liver microsomes (HLM, from 48 donors) and intestinal microsomes (HIM, prepared from the duodenum and jejunum sections of each of 5 donors) were purchased from BD Gentest. Recombinant human SULTs 1A1*1, 1A1*2; 1A2, 1A3, 2A1, 1E1, and 1B1, expressed in *Escherichia coli* were purchased from Cypex. Pooled human liver S9 fraction (HLS9, from 42 donors) and intestinal S9 (HIS9, prepared from 13 donors) were purchased from XenoTech. The protein contents were used as described in the data sheets provided by the manufacturers.

2.2 | Animals

All animal procedures were conducted in the strict adherence to the European Directive 2010/63/EU on the protection of animals

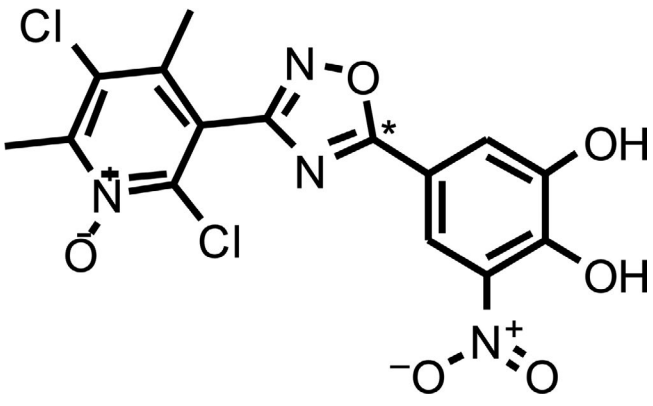

FIGURE 1 Structure of [^{14}C]-opicapone

used for scientific purposes, the Portuguese law on animal welfare (Decreto-Lei 113/2013) and the rules of the "Guide for the Care and Use of Laboratory Animals" 8th edition, 2011, Institute for Laboratory Animal Research, Washington, DC.

The animal work to evaluate the metabolite identification, mass balance, and QWBPI were conducted under the UK Home Office Project License No. PPL 70/8781, Pharmacokinetics of Pharmaceuticals. UK Home Office controls scientific procedures on animals in the UK by the issue of licenses under the Animals (Scientific Procedures) Act 1986. The regulations conform to the European Convention for the Protection of Vertebrate Animals Used for Experimental and Other Scientific Purposes (Strasbourg, Council of Europe) and achieve the standard of care required by the US Department of Health and Human Services Guide for the Care and Use of Laboratory Animals. The Home Office license governing this study strictly specifies the limit of effects on animal. The procedures described in this manuscript did not cause any effects which exceed the severity limit of the procedure.

Male rats were used for all studies. To evaluate the disposition of opicapone-related radioactivity, Wistar rats aged 6 to 7 weeks (n = 12; 223–247 g), were obtained from Charles River UK Limited. Animals were kept with special quality control (QC) diet, RM1 (Special Diet Service) mains tap water offered ad libitum. To evaluate the metabolic profiling and identification, Sprague Dawley rats (8–10 weeks and body weight 291–351 g at the time of dosing) were supplied by Charles River. The animals were acclimatized to the experimental unit for at least 9 days prior to use on the study.

To evaluate opicapone and metabolites exposure Wistar rats were obtained from Harlan, Spain (0.17–0.2 kg) and were maintained under controlled environmental conditions in a colony room (12 h light/dark cycle, room temperature 22 ± 1°C and humidity 55 ± 15%) with food and water provided ad libitum. Animals were quarantined for 1 week before dosing.

2.3 | Mass balance evaluation

Rats were orally administered with 10 mg/kg [^{14}C]-opicapone (100 μCi/kg) in 0.5% carboxymethylcellulose (CMC). For intravenous administration the dose formulation of 1 mg/kg [^{14}C]-opicapone (100 μCi/kg) in dimethyl sulfoxide, was given as a single bolus injection into the tail vein, over a period of approximately 30 s to 1 min. Serial blood samples were removed from the tail vein of each animal following oral administration at 0.25, 0.5, 1, 2, 4, 6, 8, 24, 48, and 72 h and following intravenous administration at 0.08, 0.25, 0.5, 1, 2, 4, 8, 24, 48, and 72 h post-dosing. Samples were transferred to lithium heparin tubes, centrifuged at 5°C and the collected plasma was harvested for radioactivity counting.

Urine and feces samples were collected at 6 (only for urine), 24, 48, 72, 96, and 120 h post-dose. At the time of each fecal collection each day, the metabolic cages were washed with water and the wash was retained for radioactivity analysis. From each animal, expired CO_2 was collected into two serial solvent traps containing a CO_2 absorbing solution of 2-ethoxyethanol: monoethanolamine, 7:3 (v/v). Collections of expired air were discontinued at 48 h post-dose, since it was confirmed that less than 0.5% of dose was recovered in the previous 24 h collection period. The animals were sacrificed by CO_2 narcosis and cervical dislocation at the end of the collection period and the carcasses retained for radioactivity.

2.4 | Radioactivity determination

Radioactivity was determined in a Tricarb Series liquid scintillation analyzer (PerkinElmer LAS UK Ltd). Quench correction was checked using quenched radioactive reference standards (PerkinElmer Life Sciences UK Ltd). The limit of quantification was taken as twice the background count level. Liquid samples (e.g., urine, plasma, cage wash) were counted directly in liquid scintillant. Feces and cage debris samples were homogenized in a suitable quantity of tap water. Weighed aliquots of homogenates were allowed to dry at least overnight and then combusted using a Packard Model 307 automatic sample oxidizer (PerkinElmer LAS (UK) Ltd). Carbo Sorb®E and Permafluor®E+ were used as absorbent and scintillator, respectively.

2.5 | Quantitative whole-body phosphor imaging

QWBPI was evaluated in rats following an oral dosing via gastric gavage of 10 mg/kg [^{14}C]-opicapone (200 μCi/kg) formulated in 0.5% CMC. Following administration, animals were sacrificed at 1, 4, 12, and 48 h post-dosing by carbon dioxide narcosis. Immediately prior to sacrifice, a blood sample was removed from the tail vein into a heparinized tube. Immediately after sacrifice, the animals were rapidly frozen by immersion in a mixture of hexane/solid CO_2. Blocks were bagged and stored frozen (approximately −20°C) until required for sectioning. Samples were sectioned by a Leica CM 3600 cryomicrotome (Leica Instruments GmbH) maintained at −20°C.

The 40-μm sections were collected at five sagittal whole-body sections obtained at various levels through the carcass. Sections of interest were mounted on pressure sensitive tape (TAAB Laboratories Equipment Ltd) and left in the cryostat chamber at approximately −20°C for a minimum period of 72 h or until freeze-dried. During the freeze-drying process, the dehydration cycle on the cryomicrotome was activated to prevent timed defrosts during this period. Calibration (3–19 000 nCi/g containing ^{14}C radiolabeled compound) and QC standard blocks were sectioned in an identical manner to the animal blocks. Freeze-dried sections were placed against a phosphor screen (Raytek Scientific Ltd) for an exposure period of 18 h and then radioactivity was quantified using a Fuji model FLA5000 phosphor imager system (Raytek Scientific Ltd) and Aida™ software (v3.27). For each set of whole-body images obtained, the system was calibrated with phosphor imaging standards.

2.6 | Metabolite identification and profiling

Rats were orally administered with 100 mg/kg [^{14}C]-opicapone (100 μCi/kg) in 0.2% hydroxypropyl methylcellulose (HPMC). Serial blood samples were collected by cardiac puncture into heparinized tubes at 2, 4, 8, 24, 48, 72, and 168 h post-dose. Samples were centrifuged at 5°C and the plasma was harvested for radioactivity counting. Urine and feces samples were selected based on total radioactivity data and were pooled by combining a fixed amount of each sample. The 0–6 h and 6–24 h pools were selected for urine and 0–12 h; 12–24 h and 24–48 h were selected from feces. The radioactive concentrations of each pool were measured and the prepared pools were then stored at −80°C. The plasma samples were precipitated with MeOH/ACN (50:50; v/v) and centrifuged, and the supernatant was evaporated to the dryness under N_2. The reconstituted plasma samples were injected into HPLC. The urine was mixed with 100 μl of internal standard (opicapone deuterated), was centrifuged, and injected into HPLC. The fecal homogenates were weighed mixed with H_2O/MeOH/ACN (33:33:33 v/v/v), were homogenized, centrifuged, and the supernatants were evaporated to dryness under N_2 to be reconstituted and be injected into HPLC.

Radiolabeled components in plasma, urine, or fecal samples were profiled after separation by HPLC and subsequent radiocounting analysis using the Perkin Elmer TopCount NXT system. The chromatographic separation of metabolites in plasma, urine, and feces was achieved at room temperature on an Phenomenex Synergi Polar-RP, 4 μm, 4.6 × 250 mm HPLC column using water 0.5% formic acid and acetonitrile 0.5% formic acid as mobile phases set at the flow rate of 1.0 ml/min. The high-resolution MS and MSn acquisitions were performed with a Thermo Scientific LTQ Orbitrap mass spectrometer, fitted with an electrospray ionization source. All the proposed structures of the radiopeaks associated with mass peak did not deviate more than 5 ppm from theoretical accurate mass. The mass spectrometer was set for a full scan and data- or list-dependent scan modes with mass resolution at 60 000 for the full scan. For plasma and feces, extraction efficiency and total recovery were investigated, for urine total recovery only (details of the method in Supporting Information).

2.7 | Quantification of opicapone and metabolites in rat plasma

To evaluate the opicapone and metabolites exposure in rat plasma, animals were fasted the night before administration. Opicapone (1000 mg/kg) was given orally (p.o.) as a suspension in 0.2% HPMC. Blood was collected at 1, 2, 4, 8, 24, and 48 h after dosing with heparinized syringes and kept on ice until centrifuged. Plasma was stored at less than −20°C until the analysis of opicapone and metabolites. Opicapone and metabolites were quantified in plasma samples, following protein precipitation, using a LC-MS from Agilent with negative ion detection.

2.8 | Pharmacokinetic analysis

Pharmacokinetics parameters were calculated using non-compartmental analysis from the concentration versus time profiles using Prism GraphPad Version 5 (GraphPad Software, Inc.). Results are given as mean and range and median for t_{max}. The area under plasma concentration–time curve (AUC_{0-t}) values were calculated from time zero to the last sampling time at which the concentration is at or above the limit of quantification.

2.9 | COMT activity

The characterization of the interaction of opicapone and its metabolites, BIA 9-1079, BIA 9-1100, BIA 9-1103, BIA 9-1104, and BIA 9-3752, COMT activity was investigated with rat soluble COMT as previously described.[20]

Briefly, the COMT activity was determined by using adrenaline as substrate and measuring metanephrine formed. Reaction mix (total volume of 200 μl) contained 100 μl sample (0.2 mg total protein), the opicapone metabolites (3–3000 nM) or vehicle, pargyline (100 μM), magnesium chloride (100 μM), EGTA (1 mM), s-adenosylmethionine (500 μM), and adrenaline (1000 μM) in 5 mM phosphate buffer at pH 7.8, were preincubated for 30 min at 37°C. The reactions were then started by the addition of the substrate adrenaline and carried out for 5 min at 37°C. The reaction was stopped by the addition of Perchloric acid 2 M, and the sample was kept at 2–8°C for 1 h and subsequently was centrifuged. The supernatants were then filtered and the metanephrine formed in the reaction was measured with HPLC-ED.

2.10 | Sulfate conjugation of opicapone by SULTs

The opicapone sulfate conjugations by recombinant SULTs, human liver (HLS9), and intestinal (HIS9) S9 fractions were measured after the incubation of opicapone with a mixture of 5 mM $MgCl_2$ and 0.1 mM PAPS in 50 mM phosphate buffer at pH 7.4. After a 5-min preincubation, the reaction was initiated by the addition of opicapone. Reaction mixture was incubated for up to 60 min, in a shaking water bath at 37°C and the reaction was stopped by the addition of 0.1% formic acid in acetonitrile. After a removal of the protein by centrifugation, the supernatant was filtered and was injected into an LC-MS/MS. For the screening of SULTs involved in sulfate conjugation of opicapone, the recombinant SULT1A1*1, 1A1*2, 1A2, 1A3, 2A1, 1E1, and 1B1 at the protein concentration of 40 μg/ml were incubated with 10 μM of opicapone. Rates of sulfation of opicapone were determined, in recombinant SULT1A1 (30 μg/ml), HLS9 (1 mg/ml), and HIS9 (0.4 mg/ml) fractions with opicapone concentrations ranging from 1 to 100 μM. All the preparations were evaluated for the linearity of product formation with respect to incubation time (0–240 min) and protein concentration. The kinetic analyses were performed within the linear range of time and protein concentration obtained from each cellular fraction

and recombinant enzymes. The inhibition of the sulfation of opicapone in pooled S9 fraction and SULT1A1*1 and 1A1*2 was evaluated in the presence and in the absence of acetaminophen (substrate of SULT) at the concentrations of 1, 5, 10, 50, 100, 200, 400, and 500 μM, quercetin and 2,6-dichloro-4-nitrophenol, both substrate for SULT1A1 at 0.05, 0.1, 0.5, 1, 5, 10, 50, 100 μM.

2.11 | Glucuronidation of opicapone by glucuronyltransferases

The glucuronidations of opicapone in human liver (HLM), intestinal (HIM) microsomes, and recombinant glucuronyltransferases (UGTs) were evaluated after the incubation of opicapone with 10 mM $MgCl_2$, 2 mM UDPGA, 25 μg/ml alamethicin, 5 mM saccharolactone in 50 mM phosphate buffer at pH 7.5. After a 5-min preincubation, the reaction was initiated with the addition of opicapone. Reaction mixture was incubated in a shaking water bath at 37°C for up to 60 min and the reaction was stopped by the addition 0.1% formic acid in acetonitrile. After a removal of the protein by centrifugation, the supernatant was filtered and was injected into an LC-MS.

For the screening of the recombinant enzymes involved in opicapone glucuronidation, UGTs 1A1, 1A3, 1A6, 1A7, 1A10, 2B7, 1A4, 1A8, 1A9, 2B15, 2B4, and 2B17 at the total protein concentration of 0.4 mg/ml were incubated with 20 μM of opicapone. The rates of opicapone glucuronidation in recombinant UGTs, HLM, and HIM were determined with opicapone concentrations ranging from 1 to 250 μM. The linearity of product formation with respect to protein concentration (0.025–0.8 mg/ml) was evaluated and the experimental conditions were chosen within the linearity range previously evaluated for product formation with respect to incubation time (0–60 min) and protein concentration.

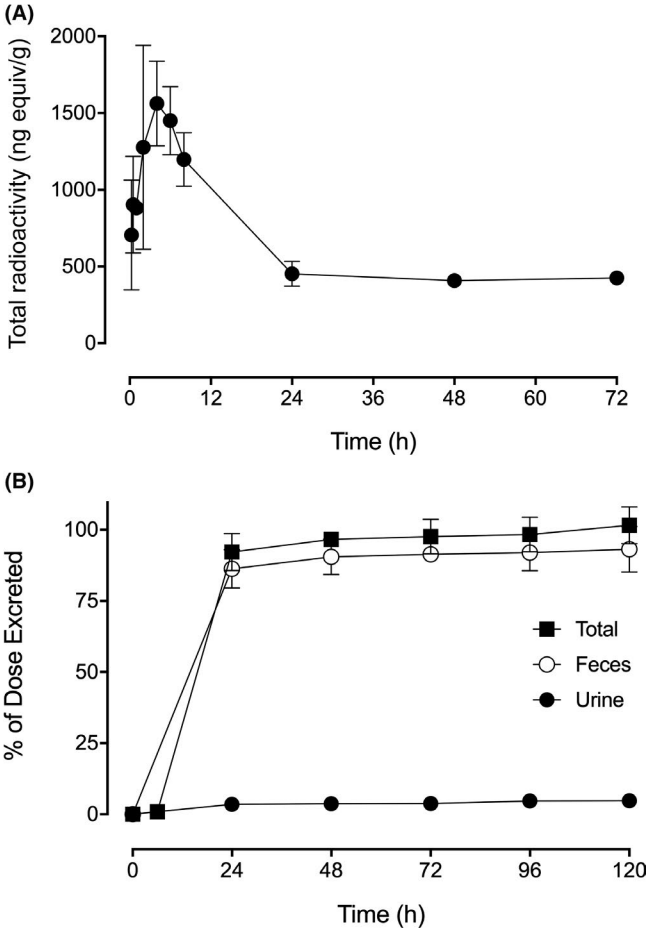

FIGURE 2 Mean plasma concentration of opicapone-related radioactivity in (A) rat plasma, (B) mean cumulative excretion of total radioactivity in urine, feces, cage wash, and cage debris from male Wistar rats following oral single dose of 10 mg/kg with 100 μCi/kg of [^{14}C]-opicapone. Each point represents mean ± *SEM* of four animals

3 | RESULTS

3.1 | Mass balance

The mean cumulative dose recovered over time in feces, urine, and the total radioactivity following an oral administration of 10 mg/kg of [^{14}C]-opicapone is shown in Figure 2. Five days (120 h) after a single oral dosing, approximately 100.7% (range from 93.3% to 108.8%) of the administered dose had been excreted, with 4.0% of the radiolabeled material excreted to urine and 92.3% excreted in feces, respectively. The majority of fecal excretion occurred in the first 24 h post-dose, representing about 86.3% of the total excretion via this route. Urinary excretion was a minor route of the elimination being approximately 23-fold less than fecal excretion (Figure 2B). As shown in Figure 2A, opicapone-related radioactivity in plasma peaked at 4 h post-dose with a maximal concentration of 1561 ng equiv/g. The peak was followed by a decline to 453 ng equiv/g at 24 h post-dose (approximately 3.5-fold less than C_{max}). The total plasma radioactivity slowly declined to an average of 426 ng equiv/g at 72 h, the last time point evaluated.

Opicapone mass balance was also evaluated in a study intended to profile and identify its metabolites (in plasma, urine, and feces) after administration of 100 mg/kg of [^{14}C]-opicapone to male Sprague Dawley rats. As described above for the dose of 10 mg/kg, following a single oral administration of [^{14}C]-opicapone of 100 mg/kg, the main route of excretion was *via* the feces, with a mean of 88.0% recovered by 168 h post-dose. Urinary excretion was minor route of the elimination accounted for 4.9% of the administered dose. The mean total recovery by 168 h post-dose including cage wash, gastrointestinal tract, and carcass, was 94.7 ± 4.2%. The plasma kinetics of total radioactivity were determined with blood samples collected from 0.5 to 168 h post-dose and levels of total radioactivity are determined in blood and plasma samples as presented in Table 1. The mean concentration of total radioactivity in plasma following single oral administration was detectable shortly after administration (T_{max} range 0.5–1 h post-dose) with a maximal concentration of 35.3 μg equiv/ml and an AUC_{0-t} of 402 μg equiv.h/ml. Total radioactivity remained quantifiable up to 168 h post-dose in all animals with a mean circulating concentration of 1.09 μg equiv/ml. Geometric mean total radioactivity whole blood to plasma concentration ratios were 0.49 at

	t_{max} (h)[a]	C_{max} (µg equiv/ml)	C_{max}/D (µg equiv/ml)/(mg/kg)	AUC_{0-t} (µg.h/ml)	AUC_{0-t}/D (µg.h/ml)/(mg/kg)
Plasma	1 (0.5–4)	35.3 (9.19)	0.353 (0.0919)	402 (65.7)	4.02 (0.657)
Whole blood	1	16.0 (4.47)	0.160 (0.0447)	259 (48.7)	2.59 (0.487)

Note: No AUC_{0-inf} and $t_{1/2}$ (h) were reported since the extrapolation of the AUC to infinity represents more than 20% of the total area.

[a]Median (min and max) is presented.

TABLE 1 Mean pharmacokinetic parameters of plasma and whole blood following a single oral administration of [^{14}C]-opicapone to male rats (n = 4)

0.5 h and 0.65 at 168 h post-dose, suggesting a similar distribution of [^{14}C]-opicapone or metabolites into whole blood cells over time, up to 168 h post-dose.

Five days following an intravenous administration of 1 mg/kg [^{14}C]-opicapone, the mean overall recovery of total radioactivity was 89.0% (range from 82.8% to 95.3%) of the administered dose, with the primary route of excretion being via hepatic excretion (Figure 3B). On average, approximately 72.8% was recovered by 5 days post-dose in feces with the majority of the fecal excretion occurring in the first 24 h post-dose (50.1%). The mean urinary excretion over 5 days post-dose was 5.7% with the majority of the urinary excretion occurring in the first 24 h. Following a single intravenous administration of [^{14}C]-opicapone, the C_{max} of total radioactivity was 11 584 ng equiv/g (Figure 3A) at the first time point collected. Thereafter, the mean concentrations decreased to 2305 ng equiv/g (approximately fivefold lower) at 1 h post-dose and by 24 h further decreased to 550 ng equiv/g. The total plasma radioactivity levels reached a mean value of 502 ng equiv/g at 72 h post-dose, the last sampling time point. In Wistar rats the amount of opicapone excreted in exhaled air was 1.5%–2.2% of the administered dose, independently of the route of administration. About 1.4% and 5.5% of the radioactivity was recovered in the carcass at the end of the collection period (120 h post-dose) after oral and intravenous dosing, respectively. The amount of radioactivity recovered in carcass following an intravenous administration was fourfold higher than that following an oral administration.

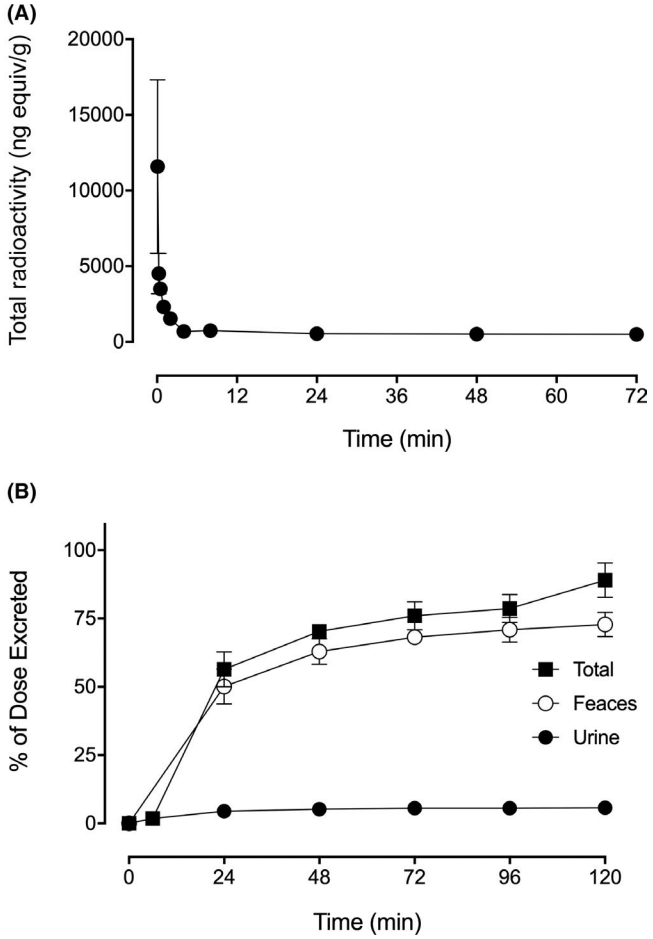

FIGURE 3 Mean plasma concentration of opicapone-related radioactivity in (A) rat plasma, (B) mean cumulative excretion of total radioactivity in urine, feces, cage wash, and cage debris from male Wistar rats following oral single intravenous of 1 mg/kg with 100 µCi/kg of [^{14}C]-opicapone. Each point represents mean ± *SEM* of four animals

3.2 | Quantitative whole-body phosphor imaging

The distribution of opicapone-associated radioactivity in whole-body sections of the animals following an oral administration of [^{14}C]-opicapone at a target dose level of 10 mg/kg was evaluated in 43 tissues at 1, 4, 12, and 48 h post administration. The absorption of radioactivity was rapid with measurable levels of radioactivity present in most tissues at 1 h post-dose with the highest tissue levels seen in the liver, kidney cortex, and kidney medulla (4387, 3457, and 3280 ng equiv/g) compared with blood concentration of 709 ng equiv/g. The maximum tissue concentrations achieved in approximately half of the tissues at 4 h post-dose.

At 12 h post-dose, radioactivity concentrations had declined with the highest levels of radioactivity associated with the liver, kidney cortex, and kidney medulla, with a tissue to blood ratios of 18.0, 11.8, and 10.4, respectively (Table S1), and with caecum and large intestine contents. At 48 h post-dose, the elimination of radioactivity was almost complete with the majority of tissues with radioactivity below the limit of quantification (129 ng equiv/g). Tissues in which radioactivity concentrations at 48 h were within twofold those at 12 h post-dose were the kidney, liver, lung, spleen, submaxillary salivary gland, thyroid, and brown fat but the exception of tissues associated with biotransformation and elimination (liver, kidney), the concentration in the other tissues at 48 h was lower than those in

blood (Table S1). Radioactivity was BLQ at all the time points in the brain, indicating that opicapone and/or its metabolites minimally distributed to the CNS. The radioactivity levels in blood measured by QWBPI were comparable to the values obtained by sample combustion of blood samples taken immediately prior to sacrifice. Blood levels at 12 h post-dose were 244 and 247 ng equiv/g by QWBPI quantification and by sample combustion.

3.3 | Opicapone metabolite identification and profile in the rat

The metabolism of [^{14}C]-radiolabeled opicapone following a single oral administration of 100 mg/kg to rats was investigated by analyzing plasma, feces, and urine samples using accurate mass spectrometry and off-line radiodetection. Representative radiochromatograms obtained from plasma collected at 4 h post-dose, from urine pool (6–24 h) and feces pool (12–24 h) are shown in Figure S1. The proposed metabolic pathway of opicapone in rats is presented in Figure 4.

In total, 12 radioactive regions were identified in plasma after an administration of opicapone. The radiopeaks corresponding to opicapone and its derivatives with synthetic reference standards such as BIA 9-1079 (*N*-oxide reduction of the pyridine 1-oxide moiety), BIA 9-1103 (3-O-sulfation), BIA 9-1106 (3-O-β-glucuronidation), BIA 9-1101 (3-O-methylation of BIA 9-1079), and the opicapone *O*-methylated conjugate at 3- and 4-positions of the nitrocatechol ring, BIA 9-1100 and BIA 9-1104, respectively, accounted for about 95% of total $AUC_{0-168\ h}$ in plasma (Table S2). Unchanged opicapone represented 15.1% of the total drug-related radioactivity exposure ($AUC_{0-168\ h}$) and it was the most abundant circulating component in the earliest time point analyzed (2 h post-dose). The major circulating metabolites included BIA 9-1101 (37.9% of $AUC_{0-168\ h}$), BIA 9-1103 (20.2% of $AUC_{0-168\ h}$), and BIA 9-1079 (12.8% of $AUC_{0-168\ h}$). BIA 9-1103 was detectable in the circulation up to 24 h post-dose, BIA 9-1079 was detectable up to 8 h, and BIA 9-1101, the 3-*O*-methylated form of BIA 9-1079, was still detectable at 168 h post-dose. The opicapone-methylated derivatives BIA 9-1100 and BIA 9-1104, were two closely eluting metabolites, with BIA 9-1100 being far more abundant, collectively accounting to 4.8% of $AUC_{0-168\ h}$, and BIA 9-1106 accounted to 4.3% of $AUC_{0-168\ h}$. As shown in Table S2, six additional radiopeaks attributed to opicapone metabolites with no synthetic reference standards were also observed. Except for the radiopeaks with the relative retention window of 19.50–20.10 min and 14.78–14.93 min where no metabolite was proposed, for all the other radiopeak detected in plasma a metabolite was tentatively proposed. These include a molecule detected in plasma with a deprotonated molecular ion at $[M\text{-}H]^-$ *m/z* of 571.0258 what was assigned to a glucuronide of BIA 9-1079 and accounted for 0.4% of total circulating radioactivity. Other glucuronide conjugates were assigned to two closely eluting deprotonated molecular ion at $[M\text{-}H]^-$ *m/z* of 585.0782 and $[M\text{-}H]^-$ *m/z* of 543.0682. Those was tentatively assigned to glucuronide conjugation of opicapone derivatives formed by *N*-oxide reduction, reduction of nitro-function, and reductive ring opening of the oxadiazole ring (M41); and to a glucuronide conjugated of M4 (derived from the N-acetylation of the reduced form of nitrocatechol of M41). They collectively accounted for 0.4% of total radioactivity. A putative isomer of M4 glucuronide was also detected, accounting for 2.3% of total circulating radioactivity. Another glucuronide conjugate with a deprotonated molecular ion at $[M\text{-}H]^-$ *m/z* of 583.0621 was assigned to an intermediate metabolite formed by *N*-oxide reduction and reduction of nitro-function of opicapone (BIA 9-3739 glucuronide). This metabolite closely eluted at relative retention window of 11.25–12.60 min, with deprotonated molecular ion at $[M\text{-}H]^-$ *m/z* of 585.0313 with a proposed formula of $C_{22}H_{19}ClN_4O_{12}S$. As the Cl isotope pattern suggested the presence of a single chlorine atom, it was proposed that this metabolite may be formed via displacement of one Cl atom with glutathione (GSH), cleavage of the resulting GSH conjugate to a sulfhydryl group, and glucuronidation. Several additional metabolites were not associated with radioactivity peak but were detected by MS. These included BIA-1104, 4-O-methylation of opicapone, and BIA 9-4584 derived from 3-O-sulfate and 4-methylation of nitrocatechol. Both confirmed by matching the retention time with reference standard spiked into the solvent.

Across the sampling period of 24 h, 16 radiopeaks were detected in urine as [^{14}C]-opicapone-related compounds (Figure S1B). None of these retention time windows represented >1% of administered radioactivity. Only low amounts of unchanged parent were observed (0.1% of the administered dose) indicating minimal renal clearance of opicapone. The most abundant metabolites observed in urine were M4 and BIA 9-1106 which represented 0.99% and 0.85% of radioactivity of the administered dose, respectively. M4 was detected in urine with a deprotonated molecular ion at $[M\text{-}H]^-$ *m/z* of 409.0473. Other observed metabolites in urine included: a glucuronide conjugate of M4 (also observed in plasma), BIA 9-3752 (a carboxylic acid nitro-reduced and N-acetylated, likely formed by hydrolysis of the oxadiazole moiety), a glucuronide conjugate of BIA 9-3752, BIA 9-1103, a glucuronide conjugate of BIA 9-1079, and a metabolite with a $[M\text{-}H]^-$ *m/z* of 585.0328 tentatively assigned to a metabolite derivative from the GSH conjugation of opicapone (also observed in plasma). Additionally, a metabolite with a $[M\text{-}H]^-$ *m/z* of 423.0171 was observed accounting to less than 0.1% of the administered dose. The proposed molecular formula for this metabolite ($C_{16}H_{13}ClN_4O_6S$) suggested the presence of a single Cl atom. As proposed for the $[M\text{-}H]^-$ *m/z* of 585.0328, this metabolite may be formed from opicapone via displacement of one of Cl atoms with GSH, followed by cleavage of the resulting GSH conjugate to a sulfhydryl group and then methylation.

In total, 48 radiopeaks corresponding to [^{14}C]-opicapone-related radioactivity were identified in feces (Figure S1C), but only 10 of them have quantified levels higher than 1% of the received dose. Opicapone, BIA 9-1079, BIA 9-3721 (a carboxylic acid metabolite likely formed by hydrolysis of the oxadiazole moiety of M41), and BIA 9-3752 (a carboxylic acid likely formed by hydrolysis of the oxadiazole moiety of M4) were confirmed by comparison of retention times with the corresponding standards synthesized. All other metabolites are putative that match with the measured sum formulas

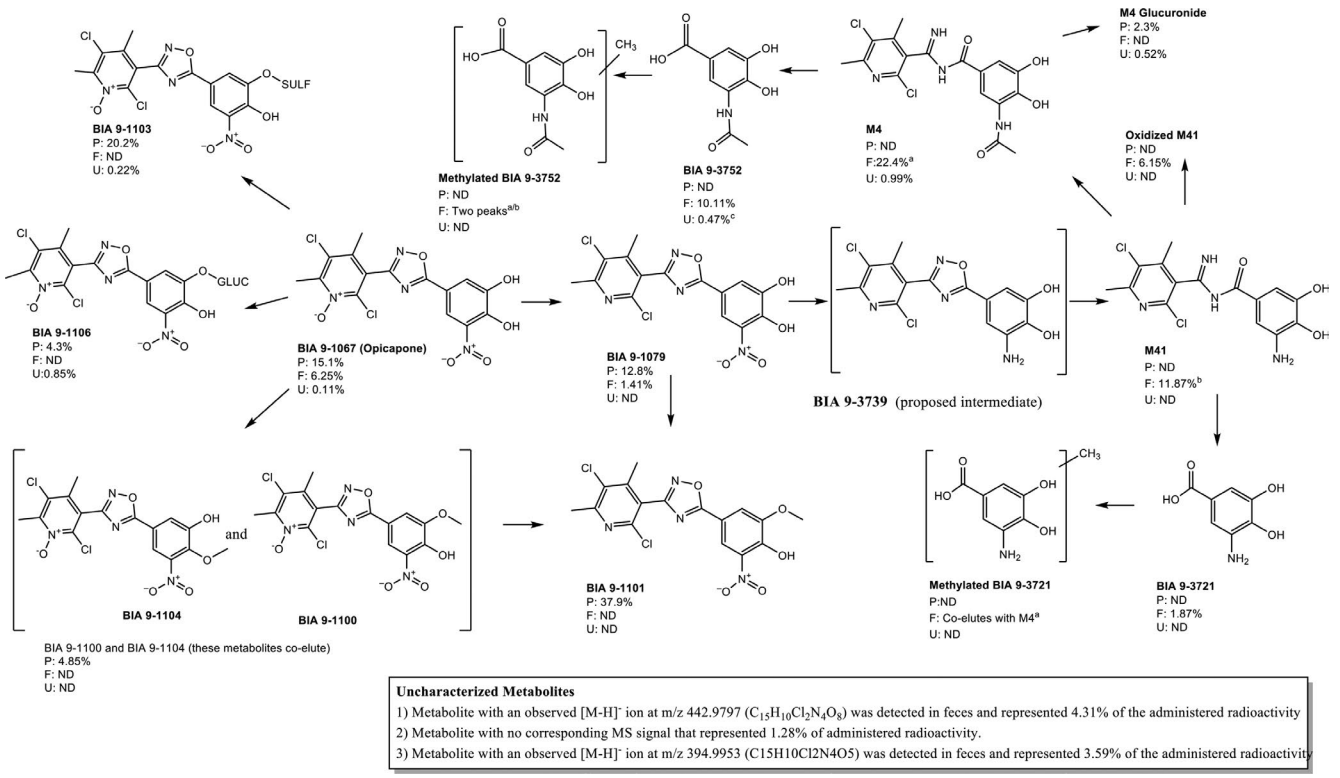

FIGURE 4 Proposed metabolic pathway for opicapone in rats

but may not correspond to the correct isomeric form. Some of the extracted ion chromatograms suggest the presence of several isomers (such as traces *m/z* 224, m/z 182, and *m/z* 365). Unchanged opicapone accounted for 6.25% of the administered radioactivity excreted in feces. As presented in Table S2, nine additional radiopeaks, some composed of multiple metabolites, were observed in the feces and collectively accounted for approximately 70% of the administered radioactivity of the administered dose. BIA 9-3721 accounted for 1.87% and BIA 9-3752 accounted for 10.11% of dose. BIA 9-1079 accounted for 1.14% and an isomer of BIA 9-1079 detected at retention time window of 13.65–14.70 min, accounted for 3.59% of the dose. Although M41 conjugated with glucuronide was detected in plasma the proposed metabolite M41 was only detected in feces. This molecule was assigned to a deprotonated molecular ion at $[M-H]^-$ *m/z* of 367.0368 with a suggested molecular formula of $C_{15}H_{14}O_3N_4Cl_2$. M41 was tentatively proposed to be formed by *N*-oxide reduction, nitro group reduction, and reductive ring opening of the oxadiazole moiety of opicapone. M41 closely co-eluted with a molecule with deprotonated molecular ion at $[M-H]^-$ *m/z* of 224.0557 and a proposed molecular formula of $C_{10}H_{11}NO_5$. This molecule was tentatively assigned to a molecule formed by the methylation of BIA 9-3762 (however, this was deemed to be the minor component in this region), that collectively with M41 accounted for 11.8% of the dose in feces. M4, also detected in urine, was closely detected in feces with a deprotonated molecular ion at $[M-H]^-$ *m/z* of 182.0452 and *m/z* 224.0557 collectively accounting for 22.4% of the administered dose. The measured accurate mass suggested a molecular formula of $C_8H_9NO_4$ and $C_{10}H_{11}NO_5$, respectively that were tentatively assigned to molecules formed by methylation of BIA 9-3721 and BIA 9-3752. An oxidized form of M41 was detected in feces with a deprotonated molecular ion at $[M-H]^-$ *m/z* of 365.0210. The measured accurate mass suggested a molecular formula of $C_{15}H_{12}O_3N_4Cl_2$ and accounted to 6.15% of the dose.

Although the extraction efficiency was close to 100% in plasma, the absolute recovery was highly variable and ranged between 42% and 81.2%. No time-dependent variation was observed in the recovery. Absolute recovery for urine pool samples was around 100% and for feces ranged between 42% and 62% in the individual pools. The recovery of radioactivity after HPLC and fraction collection was 91.8% for plasma, 96.8% for urine, and for feces was 85.9%.

3.4 | Quantification of opicapone and metabolites in rat plasma

The pharmacokinetic parameters derived from opicapone and its metabolites in rat plasma after an oral administration of opicapone (1 g/kg) are depicted in Table 2. Opicapone reached at the maximum plasma concentration (C_{max}) of 7091.0 (1032.5) ng/ml within 3 h before falling back to low levels over the next 24 h and then returning to baseline at 48 h. The AUC_{0-48} obtained for opicapone was 45 028.5 (10 925.9) ng.h/ml. Opicapone was mainly conjugated to the opicapone 3-*O*-β-glucuronide (BIA 9-1106) and opicapone 3-*O*-sulfate derivatives (BIA 9-1103). 3-*O*-sulfate derivatives reached a C_{max} within 3 h post administration and remained the major circulating metabolite over 8 h post administration. The mean AUC_{0-t} of

TABLE 2 Mean (*SD*) pharmacokinetic variables of opicapone and metabolites opicapone reduced in the N-oxide moiety (BIA 9-1079), 3-*O*-methyl-opicapone (BIA 9-1100), 3-*O*-sulfate-opicapone (BIA 9-1103), 3-*O*-sulfate-BIA 9-1079 (BIA 9-1105), and 3-*O*-glucuronide-opicapone (BIA 9-1106) in rats following oral administration of 1 g/kg of opicapone

	C_{max} (ng/ml)	t_{max} (h)	AUC_{0-t} (ng.h/ml)
Opicapone	7091.0 (1032.5)	3 (2–4)	45 028.5 (10925.9)
BIA 9-1079	381.3 (87.5)	4 (2–8)	4085 (1403.0)
BIA 9-1103	3748.5 (1765.5)	3 (2–4)	32 580.3 (17290.9)
BIA 9-1106	4294.2 (820.9)	2 (2–4)	27 642.5 (10759.5)
BIA 9-1100	1420.7 (427.7)	1.5 (1–4)	7921.5 (2064.6)
BIA 9-1105	58.2 (32.6)	16 (8–24)	1322.5 (503.5)

Note: AUC_{0-t}, area under the plasma concentration-time curve from time zero to the last sampling time at which the concentration was detected; C_{max}, maximum plasma concentration; t_{max}, time to maximum plasma concentration.

opicapone sulfate (BIA 9-1103) was 32 580.3 (17 290.9) ng.h/ml. 3-*O*-glucuronide derivative (BIA 9-1106) derivatives reached the maximal concentration within 2 h post administration and remained the second major circulating metabolite of opicapone over 8 h post administration. The mean AUC_{0-t} of opicapone glucuronide was 27 642.5 (10 759.5) ng.h/ml. At 24 h post-dose no opicapone sulfate and glucuronide were detected in the circulation. Low levels of other opicapone derivatives BIA 9-1079 (resulting from the reduction at the dimethylpyridine 1-oxide moiety), BIA 9-1079 sulfate (BIA 9-1105), and BIA 9-1100 (the *O*-methylated conjugate at position 3) were quantified in rat plasma and only traceable amounts of BIA 9-1079 glucuronide (BIA 9-1107) were also detected in circulation.

3.5 | COMT activity

The potential modulatory effect of the identified metabolites (BIA 9-1079, BIA 9-1100, BIA 9-1103, BIA 9-1104, and BIA 9-3752) in COMT activity was investigated with rat soluble COMT in the presence of 3000 nM opicapone metabolites. While BIA 9-1100, BIA 9-1103, and BIA 9-3752 had no modulatory effect upon the activity of the enzyme up to concentrations of 3000 nM, BIA 9-1079, and BIA 9-1104 were active in inhibiting the enzyme at the concentration. Further incubations of increased concentrations of opicapone, BIA 9-1079, and BIA 9-1104 with rat soluble COMT resulted in a concentration-dependent reduction of COMT activity and the IC_{50} values derived from the respective inhibitory curves were, respectively, 224, 128, and 429 nM.

3.6 | In vitro opicapone sulfation by SULTs

The kinetic analyses of opicapone sulfate conjugation were evaluated using pooled HLS9 and HIS9 fractions. As presented in Table S3, the apparent kinetic parameters fitted to Michaelis–Menten equation with an apparent K_m value of 8.2 ± 1.1 μM and 20.5 ± 2.6 μM, for HIS9 and HLS9 fractions, respectively. The apparent K_m value in HLS9 was approximately twofold higher than that in HIS9. The intrinsic clearance ($Cl_{int} = V_{max}/K_m$) calculated for HIS9 was 0.1662 μl/mg protein/min and for HLS9 was 0.01795 μl/mg protein/min. From the tested SULTs only SULT 1A1 polymorphs *1 and *2 produced significant amounts of 3-*O*-sulfate-opicapone (11.7 ± 1.8 and 19.1 ± 1.8 pmol/mg protein/min, respectively). SULT1A2, 1A3, 2A1 1E1, and SULT1B1 produced small amounts of 3-*O*-sulfate-opicapone (between 0.03 and 0.4 pmol/mg protein/min) (Figure 5A). The kinetics of opicapone sulfation by SULT1A1*1 and 1A1*2 are presented in Table S3. SULT1A1*1 and 1A1*2 had similar affinities for the conjugation of opicapone, as shown by the apparent K_m values of 18.7 ± 11.0 μM and 27.3 ± 22.3 μM, respectively. No inhibition was observed upon the sulfate conjugation of opicapone in the presence of acetaminophen but quercetin and 2,6-dichloro-4-nitrophenol completely inhibited the sulfate conjugation of opicapone in HLS9, HIS9, and SULT1A1 (IC50 presented in Table S5).

3.7 | In vitro opicapone glucuronidation

The kinetic analyses of opicapone glucuronidation were performed in HLM and HIM. As depicted in Table S4, the apparent kinetic parameters were calculated for HIM and HLM fractions, with an apparent K_m value of 41.9 ± 26.9 μM and 27.9 ± 6.4 μM, respectively. The apparent V_{max} values were 4.5-fold higher in HIM than that in HLM, whereas K_m values in the intestinal microsomes did not markedly differ from those in liver microsomes. The calculated intrinsic clearance ($Cl_{int} = V_{max}/K_m$) was threefold higher in HIM than that in HLM, respectively, with 4.5 μl.mg protein/min and 1.5 μl/mg protein/min. Twelve commercially available UGTs were used to evaluate their ability to conjugate opicapone to 3-*O*-glucuronide-opicapone. From the tested UGTs, 1A7, 1A8, 1A9, and 1A10 produced significant amounts of 3-*O*-glucuronide-opicapone (more than 500 pmol/mg protein/min). UGT 1A1, 1A3, 2B7, 2B15, 1A6 produced little amounts of BIA 9-1106. No metabolite formation was detected over an incubation period of 60 min in UGT1A4, 2B4, and 2B17 (Figure 5B). The characterization of opicapone glucuronidation kinetics was performed for UGTs 1A1, 1A3, 1A6, 1A7, 1A8, 1A9, 1A10, and 2B7 and determined parameters are listed in Table S4. There is a rather considerable range of the affinities for the conjugation of opicapone as shown by the apparent K_m values determined. The isoform with the highest affinity was UGT 1A7, with a Km of 1.8 ± 0.5 μM, followed by UGT 1A9, 1A1, and 2B7 with Km values of 13.7 ± 6.7 μM, 18.0 ± 2.9 μM, and 20.6 ± 4.4 μM, respectively. UGT1A6-mediated glucuronidation was linear for the concentrations tested and UGTs 1A8 and 1A10 had apparent K_m of 34.8 ± 9.6 μM and 64.9 ± 23.8 μM, respectively. The UGT with lower glucuronidation affinity of opicapone was UGT 1A3 with a Km of 213.0 ± 34.3 μM.

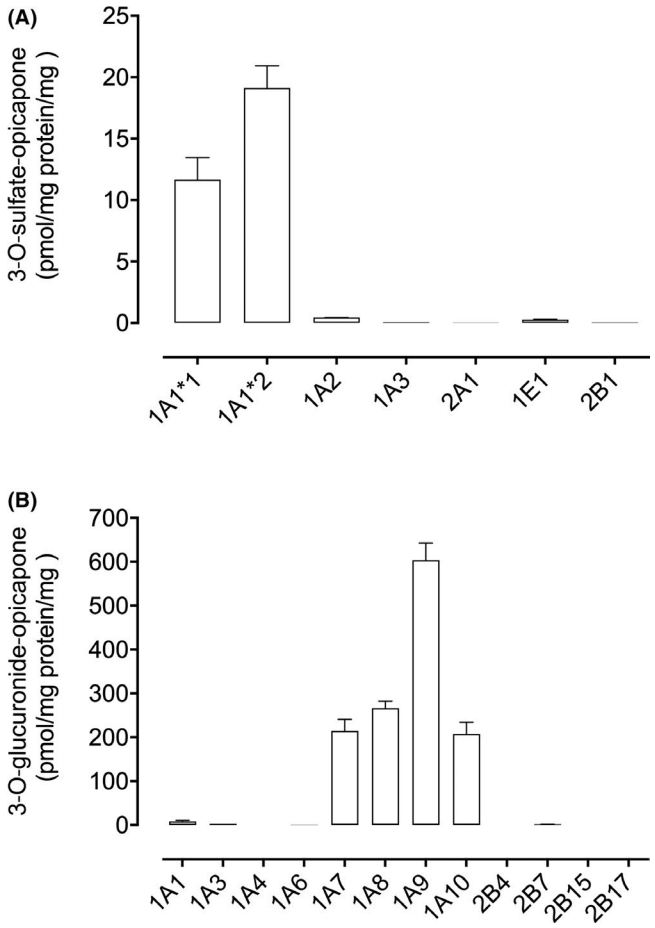

FIGURE 5 Apparent sulfation rates catalyzed by recombinant human sulfotransferase (0.4 mg/ml) isoforms. Rates were determined at 10 μM opicapone. Values represent means ± *SEM* of two determinations (A); apparent glucuronidation rates catalyzed by recombinant human uridine 5'-diphospho-glucuronosyltransferase isoforms. Rates were determined at 20 μM opicapone. Values represent mean ± *SEM* of two determinations (B)

4 | DISCUSSION AND CONCLUSIONS

Following the oral administration of [^{14}C]-opicapone to rats the recovery of the radioactivity was almost completed after 120 h post-dose. The main route of excretion was via feces, accounting for more than 88% of the administered dose and the urinary excretion as a minor pathway, accounted for less than 5% of the administered dose. The intravenous administration of [^{14}C]-opicapone confirmed the biliary excretion as the main route of the systemic elimination of the radioactivity in the rat, with around 72% of total radioactivity quantified in feces. Excretion was biphasic, with a rapid elimination over the first 24 h, followed by a slow elimination up to 120 h. Additionally, QWBPI showed that [^{14}C]-opicapone was rapidly absorbed, distributed, and was eliminated from the majority of rat tissues, with almost complete elimination after 48 h post-dosing. With the exception of the liver and kidney, that showed a tissue to blood ratio significantly higher than one at 48 h the majority of tissues showed no quantifiable levels of the radioactivity. Again, QWBPI data suggest a slower elimination of opicapone-related radioactivity from organs generally associated to the metabolism and elimination reflecting the biphasic excretion with a slow elimination phase. Furthermore, the data from the QWBPI evaluation demonstrate essentially no CNS penetration of opicapone-related radioactivity, further confirming that opicapone is a peripheral COMT inhibitor.[1]

By increasing 10-fold the dose to 100 mg/kg [^{14}C]-opicapone the recovery, mainly in feces, was almost completed after 168 h, with the radioactivity still quantifiable up to 168 h post-dose in all animals, corroborating the slow elimination of opicapone-related radioactivity in the rat. In plasma unchanged opicapone accounted for 15.1% of the total drug-related material ($AUC_{0-168\ h}$), peaking at 2 h post-dosing and decline to below limit of detection after 24 h. The main metabolic conversions of opicapone were observed at the nitrocatechol moiety such as sulfate-, glucuronide-, methyl-conjugations, and the reduction of nitro-function. In addition, various other combinations of these conversions with *N*-oxide reduction at the 2,5-dichloro-4,6-dimethylpyridine 1-oxide moiety, N-acetylation on the reduced nitro-function, reductive cleavage of 1,2,4-oxadiazole ring, opening ring, and the subsequent production of several ring-opened products were proposed, as presented in metabolic scheme for the metabolism of opicapone (Figure 4). The observation of trace thiol derivatives in plasma and urine, suggests a possible downstream GSH adduct of opicapone as metabolite. Opicapone sulfate (BIA 9-1103), the *N*-oxide reduced form (BIA 9-1079), and the methylated form of *N*-oxide reduced opicapone (BIA 9-1101) were the only components observed at mean levels greater than 10% of total circulating radioactivity, collectively accounting for 71% of the total drug-related material. From these metabolites only BIA 9-1079 was shown to be an active metabolite (IC_{50} of 128 nM) which may contribute, together with opicapone, to the COMT inhibition in vivo. The remaining radioactivity was attributed to multiple minor metabolites. Both BIA 9-1103 and BIA 9-1101 plasma exposure exceeded that of the parent opicapone (20.2% and 37.9% vs. 15.1%) but only BIA 9-1101 was detectable in circulation up to 168 h post-dose, which definitely contributes to the long plasma elimination of opicapone-related radioactivity observed. Long lasting methyl derivatives of COMT inhibitors have been described before.[21]

The opicapone-methylated derivatives (BIA 9-1100 and BIA 9-1104) and the glucuronide conjugates of opicapone (BIA 9-1106) showed low circulating levels, each one accounted for less than 5% of total radioactivity. Interestingly, only the opicapone-methylated derivative BIA 9-1104, but not BIA 9-1100, was shown to be endowed with activity in inhibiting COMT.

Although metabolites resulting from secondary or multiple reductive reactions from *N*-oxide reduced form of opicapone were detected in the circulation, the main reductive metabolic pathways of opicapone were detected in feces, as indicated in the metabolism scheme shown in Figure 4. The most common reductive biotransformations involved in *N*-oxide reduction, nitro group reduction, and reductive opening of the 1,2,4-oxadiazole moiety followed by a hydrolytic cleavage. The most abundant metabolites were observed in feces including M41, which accounted for

approximately 12% of the administered dose, M4 (*N*-acetylated M41), which accounted for approximately 22% of the administered dose, and BIA 9-3752 (a carboxylic acid likely formed by hydrolysis of the oxadiazole moiety of M41), which accounted for approximately 10% of the administered dose. The parent compound represented 6.25% of total dose. Interestingly, none of the metabolites identified in the feces were associated with metabolites observed in the plasma, which together with the low levels of opicapone in feces suggest that opicapone was metabolized in the gastrointestinal tract mainly via reductive reactions. In gut those reactions could be promoted by gut microbiota. This is further supported by recent clinical investigations of the impact of gut microbiota on drug metabolism.[22] As a low solubility compound belonging to Biopharmaceutics Classification System class II-drugs (unpublished information), it is expected that opicapone has a prolonged residence in the gastrointestinal tract with higher concentrations in the colon, which may foster the local metabolism of opicapone. A recent publication from Vaes et al.[23] showed that among several drugs with varying BCS classification, those in BCS-class II were more likely to reach the colon and contact with microbiota. The reductive ring opening of the oxadiazole moiety of opicapone, was in line with previous studies showing the reductive cleavage of 1,2,4-oxadiazole ring-opening followed by hydrolysis resulting in the formation of carboxylic acids and amides.[24,25] In the case of opicapone no amide-related metabolite has been found although several carboxylic acids derivatives were detected in feces. The carbon dioxide collected in the exhaled air (1.5%–2.2% of the administered dose) may be a result of the hydrolysis of the carboxylic acid formed after the reductive cleavage of 1,2,4-oxadiazole ring.

A minor metabolic route also proposed may arise via nucleophilic attack with a displacement of a single chorine atom by GSH, subsequently cleaved into a sulfhydryl group. Minor levels of these metabolites were detected in plasma (<1.2% of $AUC_{0-168\,h}$) and urine (<0.3% of the dose). The replacement of a chorine, consistent with a full scan spectrum with characteristic ^{35}Cl:^{37}Cl ratio may occur via a nucleophilic aromatic substitution reaction of the chlorine atom by GSH at the C-2 position of the 2,5-dichloro-4,6-dimethylpyridine 1-oxide moiety of the opicapone molecule. The reaction is fostered by the *N*-oxide group. Interestingly, only a methyl or glucuronide conjugate of a thiol derivative was identified, and no radiopeaks associated with a GSH conjugate of opicapone were detected. This data suggest that opicapone GSH conjugate may undergo a sequential removal of glutamyl and glycyl moieties to form a cysteine conjugate and then be biodegraded into a thiol providing evidence of the mercapturic acid pathway being involved as a minor pathway in the metabolism of opicapone in the rat. Thiol derivatives are common biotransformation products of cysteine conjugates[26]

Following an oral administration of high levels of opicapone (1000 mg/kg), low levels of *N*-oxide reduced form of opicapone (BIA 9-1079) and 3-*O* methyl opicapone (BIA 9-1101) were quantified in rat plasma; however, the 3-O-glucuronidation of opicapone together with 3-O-sulfation of opicapone becomes a relevant metabolic pathway in the metabolism of opicapone in the rat. In humans at the therapeutic dose of 50 mg, although *N*-oxide reduced form of opicapone (BIA 9-1079), 3-O-glucuronidation of opicapone (BIA 9-1106), and 3-*O*-methyl opicapone (BIA 9-1101) were detected, the major circulating metabolite was 3-*O*-sulfate derivative of opicapone (BIA 9-1103).[14] Despite the differences in relative abundances being observed for those metabolites quantified in humans, they are qualitatively similar between both species, rat and human. The reaction phenotyping studies indicated that SULT 1A1 polymorphs *1 and *2 were able to sulfate opicapone and that uridine-diphosphate glucuronosyl transferase (UGT) isoforms UGT1A7, UGT1A8, UGT1A9, and UGT1A10 had the highest glucuronidation rates of opicapone.

In conclusion, opicapone, in the rat, was found to be rapidly absorbed, widely distributed to peripheric tissues, was metabolized mainly via conjugative pathways at the nitro catechol ring, and was primarily excreted to feces via bile. Moreover, the data generated in this study showed a recovery of ^{14}C after administration of [^{14}C]-opicapone to rats and qualification of the human metabolites in a preclinical specie used in opicapone toxicology assessment, supporting the regulatory filling and the marketing authorization of opicapone.

ACKNOWLEDGMENT

BIAL—Portela & C^{a}, S.A. supported this study.

DISCLOSURE

All authors have completed the Unified Competing Interest form at www.icmje.org/coi_disclosure.pdf (available upon request from the corresponding author) and declare: all were employees of BIAL—Portela & C^{a}, S.A. in the previous 3 years.

AUTHOR CONTRIBUTIONS

Participated in research design: Ana I. Loureiro, Maria João Bonifácio, Patricio Soares-da-Silva. Conducted experiments: Ana I. Loureiro, Carlos Fernandes-Lopes, Filipa Sousa. Contributed new reagents or analytic tools: László E. Kiss. Performed data analysis: Ana I. Loureiro. Wrote or contributed to the writing of the manuscript: Ana I. Loureiro, Maria João Bonifácio, Patricio Soares-da-Silva.

ETHICS STATEMENT

Procedures on animals using radiolabeled opicapone were conducted under the UK Home Office Project License No. PPL 70/8781, Pharmacokinetics of Pharmaceuticals. Procedures on animals using opicapone were approved by the Direção Geral de Veterinária, Portugal, and performed in accordance with institutional animal care guidelines. In vitro cell-free studies did not utilize human biospecimens or patient identifiable data; thus, neither approval from the ethics committee nor informed consent was required.

DATA AVAILABILITY STATEMENT

The authors confirm that the data supporting the finding on this study are available from the corresponding author upon reasonable request.

REFERENCES

1. Bonifacio MJ, Torrao L, Loureiro AI, Palma PN, Wright LC, Soares-da-Silva P. Pharmacological profile of opicapone, a third-generation nitrocatechol catechol-O-methyl transferase inhibitor, in the rat. *Br J Pharmacol*. 2015;172:1739-1752.
2. Kiss LE, Ferreira HS, Torrao L, et al. Discovery of a long-acting, peripherally selective inhibitor of catechol-O-methyltransferase. *J Med Chem*. 2010;53:3396-3411.
3. Bonifacio MJ, Sutcliffe JS, Torrao L, Wright LC, Soares-da-Silva P. Brain and peripheral pharmacokinetics of levodopa in the cynomolgus monkey following administration of opicapone, a third generation nitrocatechol COMT inhibitor. *Neuropharmacology*. 2014;77:334-341.
4. Cabreira V, Soares-da-Silva P, Massano J. Contemporary options for the management of motor complications in Parkinson's disease: updated clinical Review. *Drugs*. 2019;79:593-608.
5. Fabbri M, Ferreira JJ, Lees A, et al. Opicapone for the treatment of Parkinson's disease: a review of a new licensed medicine. *Mov Disord*. 2018;33:1528-1539.
6. Fackrell R, Carroll CB, Grosset DG, et al. Noninvasive options for 'wearing-off' in Parkinson's disease: a clinical consensus from a panel of UK Parkinson's disease specialists. *Neurodegener Dis Manag*. 2018;8:349-360.
7. Ferreira JJ, Lees A, Rocha JF, Poewe W, Rascol O, Soares-da-Silva P. Long-term efficacy of opicapone in fluctuating Parkinson's disease patients: a pooled analysis of data from two phase 3 clinical trials and their open-label extensions. *Eur J Neurol*. 2019;26(7):953-960.
8. Ferreira JJ, Lees AJ, Poewe W, et al. Effectiveness of opicapone and switching from entacapone in fluctuating Parkinson disease. *Neurology*. 2018;90:e1849-e1857.
9. Castro Caldas A, Teodoro T, Ferreira JJ. The launch of opicapone for Parkinson's disease: negatives versus positives. *Expert Opin Drug Saf*. 2018;17:331-337.
10. Lees A, Ferreira JJ, Rocha JF, et al. Safety profile of opicapone in the management of Parkinson's disease. *J Parkinsons Dis*. 2019;9:733-740.
11. Rodrigues FB, Ferreira JJ. Opicapone for the treatment of Parkinson's disease. *Expert Opin Pharmacother*. 2017;18:445-453.
12. Salamon A, Zadori D, Szpisjak L, Klivenyi P, Vecsei L. Opicapone for the treatment of Parkinson's disease: an update. *Expert Opin Pharmacother*. 2019;20:2201-2207.
13. Almeida L, Rocha JF, Falcao A, et al. Pharmacokinetics, pharmacodynamics and tolerability of opicapone, a novel catechol-O-methyltransferase inhibitor, in healthy subjects: prediction of slow enzyme-inhibitor complex dissociation of a short-living and very long-acting inhibitor. *Clin Pharmacokinet*. 2013;52:139-151.
14. Rocha JF, Almeida L, Falcao A, et al. Opicapone: a short lived and very long acting novel catechol-O-methyltransferase inhibitor following multiple dose administration in healthy subjects. *Br J Clin Pharmacol*. 2013;76:763-775.
15. Lautala P, Ethell BT, Taskinen J, Burchell B. The specificity of glucuronidation of entacapone and tolcapone by recombinant human UDP-glucuronosyltransferases. *Drug Metab Dispos*. 2000;28:1385-1389.
16. Lautala P, Kivimaa M, Salomies H, Elovaara E, Taskinen J. Glucuronidation of entacapone, nitecapone, tolcapone, and some other nitrocatechols by rat liver microsomes. *Pharm Res*. 1997;14:1444-1448.
17. Loureiro AI, Bonifacio MJ, Fernandes-Lopes C, Almeida L, Wright LC, Soares-Da-Silva P. Human metabolism of nebicapone (BIA 3–202), a novel catechol-o-methyltransferase inhibitor: characterization of in vitro glucuronidation. *Drug Metab Dispos*. 2006;34:1856-1862.
18. Wright LC, Maia J, Loureiro AI, Almeida L, Soares-Da-Silva P. Pharmacokinetics, disposition, and metabolism of [^{14}C]-nebicapone in humans. *Drug Metab Lett*. 2010;4:149-162.
19. Runge-Morris M, Kocarek TA. Regulation of sulfotransferase and UDP-glucuronosyltransferase gene expression by the PPARs. *PPAR Res*. 2009;2009:728941.
20. Bonifacio MJ, Vieira-Coelho MA, Soares-da-Silva P. Kinetic inhibitory profile of BIA 3–202, a novel fast tight-binding, reversible and competitive catechol-O-methyltransferase inhibitor. *Eur J Pharmacol*. 2003;460:163-170.
21. Bonifacio MJ, Loureiro AI, Torrao L, et al. Species differences in pharmacokinetic and pharmacodynamic properties of nebicapone. *Biochem Pharmacol*. 2009;78:1043-1051.
22. Wilkinson EM, Ilhan ZE, Herbst-Kralovetz MM. Microbiota-drug interactions: impact on metabolism and efficacy of therapeutics. *Maturitas*. 2018;112:53-63.
23. van de Steeg E, Schuren FHJ, Obach RS, et al. An ex vivo fermentation screening platform to study drug metabolism by human gut microbiota. *Drug Metab Dispos*. 2018;46:1596-1607.
24. Gu C, Elmore CS, Lin J, et al. Metabolism of a G protein-coupled receptor modulator, including two major 1,2,4-oxadiazole ring-opened metabolites and a rearranged cysteine-piperazine adduct. *Drug Metab Dispos*. 2012;40:1151-1163.
25. Tsalta CD, Madatian A, Schubert EM, et al. Metabolism of [^{14}C] GSK977779 in rats and its implication with the observed covalent binding. *Drug Metab Dispos*. 2011;39:1620-1632.
26. Levsen K, Schiebel HM, Behnke B, et al. Structure elucidation of phase II metabolites by tandem mass spectrometry: an overview. *J Chromatogr A*. 2005;1067:55-72.

SUPPORTING INFORMATION

Additional supporting information may be found in the online version of the article at the publisher's website.

How to cite this article: Loureiro AI, Fernandes-Lopes C, Bonifácio MJ, Sousa F, Kiss LE, Soares-da-Silva P. Metabolism and disposition of opicapone in the rat and metabolic enzymes phenotyping. *Pharmacol Res Perspect*. 2022;10:e00891. doi:10.1002/prp2.891